FAR-INFRARED AND SUBMILLIMETER OBSERVATIONS OF INTERSTELLAR CLOUDS

Gary Melnick
Harvard-Smithsonian Center for Astrophysics
60 Garden Street
Cambridge, MA (USA) 02138

I. INTRODUCTION

This paper reviews a number of ways in which the results of far-infrared and submillimeter (FIR/SMM) observations ($50\,\mu m \leq \lambda \leq 1mm$) have been used to address some of the important questions in astrochemistry. On scales of kiloparsecs these might include questions of abundance gradients; on scales of parsecs these might include questions about the chemical structure of molecular clouds; and on scales of tenths of parsecs or less, these might include questions about chemical processing in shocks.

Because this symposium brings together workers from a wide variety of disciplines, it is instructive to first briefly review the types of transitions that give rise to the strongest lines in the FIR/SMM along with some of the problems that have limited our progress. Brevity requires that only spectroscopic studies of the interstellar gas be considered here, though it should be noted that extensive spectroscopic studies have been made of the dust continuum, many of which show interesting grain features (see Willner 1984, for a review).

In general, spectroscopic features in the FIR/SMM are dominated by transitions from species that fall into three categories: (1) atoms and atomic ions, (2) metal hydrides, and (3) heavy molecules. Examples of the first category include ground-state fine-structure transitions of OI, CI, CII, OIII, and NIII. Examples of the the second category include some of the more abundant metal-hydrogen pairs, such as OH and CH, whose lowest rotational transitions occur in the submillimeter region. The most studied of the heavy molecules shortward of 1mm is CO. Though the lowest rotational levels of CO are at millimeter wavelengths, a number of upper rotational levels have been detected between the $J = 3 \rightarrow 2$ transition at $867.00\,\mu m$ and the $J = 34 \rightarrow 33$ transition at $77.06\,\mu m$. The richness of the FIR/SMM spectrum in these lines is shown in Figure 1.

Since the optical depth due to dust is usually negligible beyond $50\,\mu m$, these transitions have been used to study regions of great visual

M. S. Vardya and S. P. Tarafdar (eds.), Astrochemistry, 137–152.

obscuration, such as star forming regions and the galactic center. Likewise, the interpretation of FIR/SMM line strengths is often more straightforward than that of their optical and near-infrared counterparts since the correction of line intensities for the effects of dust extinction are not necessary.

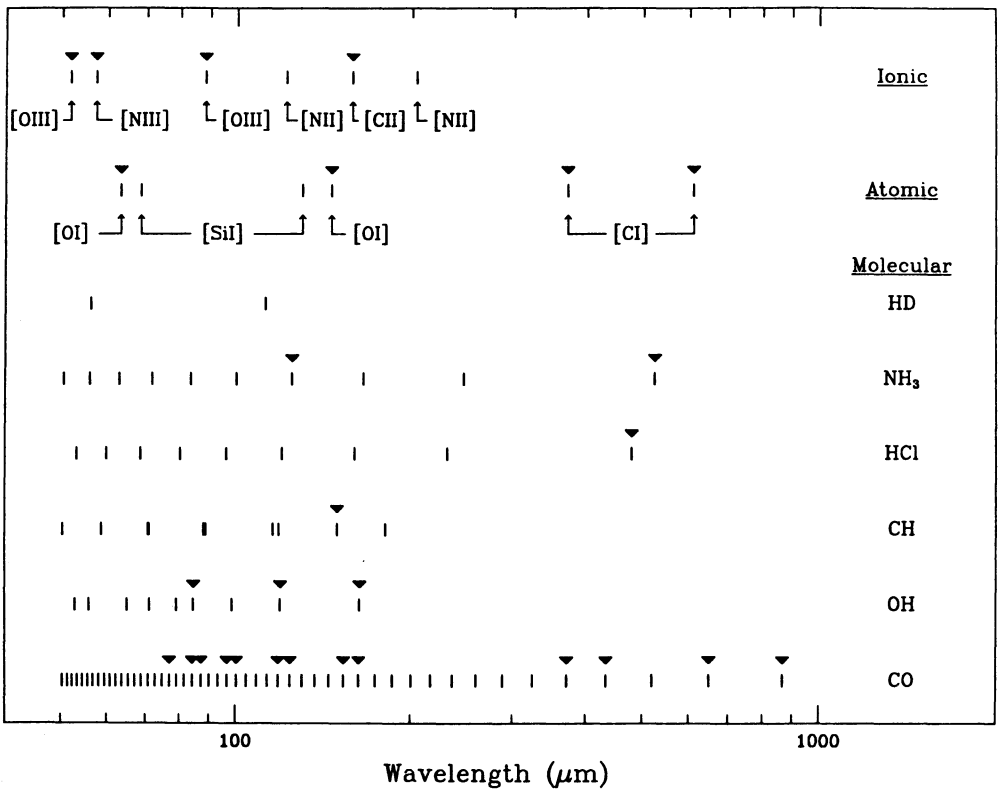

Figure 1. Some of the brightest lines occuring in the far-infrared and submillimeter region. The doublet transitions of OH and CH and the inversion-rotation transitions of NH_3 are closely spaced (on this scale) and are shown as single lines. Marked (▼) transitions have been detected as of the end of 1985.

Unfortunately, exploration of this spectral region has been limited by poor atmospheric transmission between about 14 and 700 μm, the unavailability of telescopes with apertures larger than 1 meter, and relatively brief observing periods. Due mainly to the presence of a large number of pressure broadened atmospheric H_2O rotational transitions, ground-based observers are forced to work within approximately a half dozen narrow "windows" between 1.1 and 20 μm. As shown in Figure 2, longward of 20 μm, the atmospheric transmission from even mountaintop

https://doi.org/10.1017/S0074180900153951 Published online by Cambridge University Press

altitudes is very low. For this reason, NASA has modified two aircraft, a Lear Jet and a C-141, to house a 30-cm and a 91-cm diameter telescope, respectively. The Lear Jet Observatory (LJO) and the C-141, better known as the Kuiper Airborne Observatory (KAO), permit the observer to routinely operate above about 99 percent of the terrestrial water vapor at altitudes between 41,000 and 45,000 ft. Above the tropopause pressure broadening is considerably reduced and the atmospheric transmission between residual water absorption lines is often close to 100 percent.

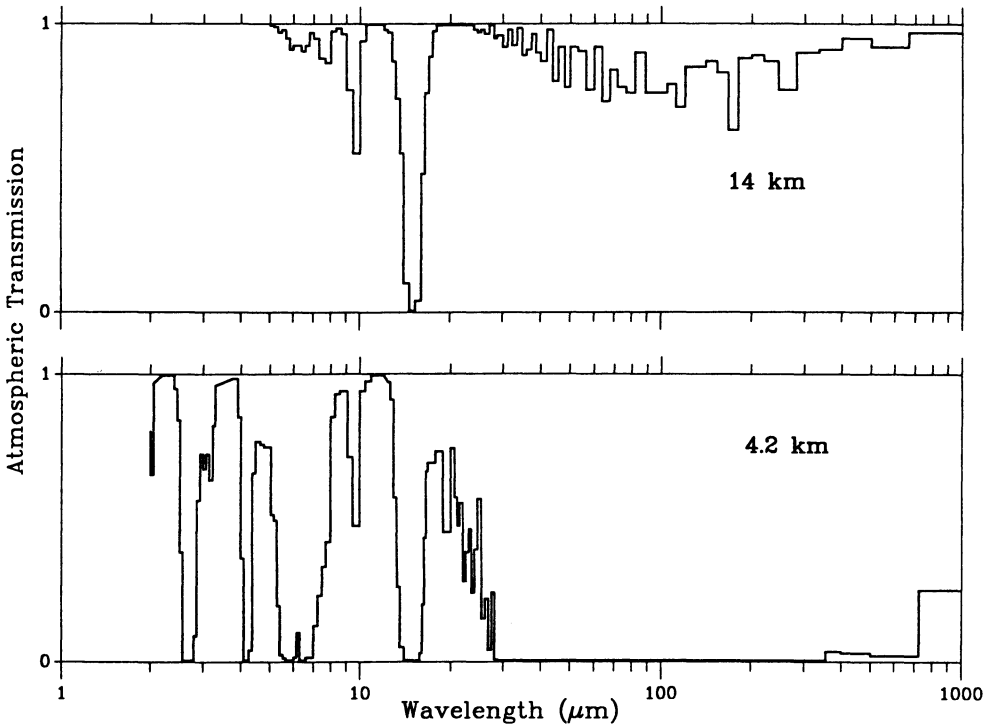

Figure 2. Atmospheric transmission at mountaintop (4.2 km) and airplane (14 km) altitudes (after Traub and Stier, 1976).

To date, the KAO is the largest observing platform capable of frequent observing above the tropopause. However, use of a 91-cm telescope means that spatial features smaller than about 1/2 arc-minute at 100 μm and 3 arc-minutes at 600 μm are inaccessible at present. Further, since only about 1/3 of the 80 flights per year program on the KAO is dedicated to FIR/SMM spectroscopy and because no more than 6.5 hours per flight can be used for observations, the total observing time available for FIR/SMM spectroscopy is the ground-based astronomer's equivalent of about 14 "clear," 12-hour nights per year. In spite of these limitations, progress has been made. Ten years ago, only one line had been

https://doi.org/10.1017/S0074180900153951 Published online by Cambridge University Press

detected between 50 μm and 1mm - the [OIII] 88.35 μm line (Ward et al. 1975). Since then, approximately 30 ionic, atomic, and molecular transitions have been observed (see Figure 1) in a variety of galactic HII regions, the galactic center, and in other galaxies.

Because of these advances, it is no longer possible to review all of the spectral work done between 50 μm and 1mm in a few pages. For this reason, three representative areas of on-going research bearing on topics closely related to astrochemistry will be discussed: (1), the N/O abundance ratio as a function of galactic radius, (2), conditions at the surface of molecular clouds and the chemical profile of molecular clouds, and (3), conditions in post-shocked gas.

II. N/O SURVEY OF THE GALACTIC DISK

The question of the nitrogen-to-oxygen abundance ratio is an interesting one not only because these two abundant elements are major coolants of the gas, but also because they are synthesized by different nuclear processes. Whereas ^{16}O is produced within massive stars and injected into the the interstellar medium via supernovae, ^{14}N is produced by the CNO cycle in low mass stars and transferred to the interstellar medium through stellar winds and planetary nebulae. Thus, since the production of ^{14}N via the CNO cycle depends on previously synthesized C and O, the relative abundance of N and O is a measure of the number of times a sample of material has been cycled through stars and on the relative number of high and low mass stars in previous generations.

Recently, Lester, Dinerstein, and their co-workers have undertaken a study of the N/O abundance ratio in a number of luminous HII regions between the galactic center and a galactic radius, R_G, of 12 kpc (Lester et al. 1983; Dinerstein et al. 1984). Unlike previous studies, which employed optical lines of O^+ and N^+ to derive the N/O ratio, Lester, Dinerstein, and co-workers used the O^{++} 51.82 and 88.35 μm and the N^{++} 57.34 μm ground-state fine-structure emission lines (see Figure 3).

As discussed by Lester et al., the expectation that $N^{++}/O^{++} \sim N/O$ is based on two assumptions - that the N^{++} and O^{++} Strömgren spheres are coincident and that within the regions observed, N^{++} and O^{++} are the dominant ions of each element. The first assumption is supported both by models of HII regions which indicate that the ionization of N and O track each other over a wide range of stellar effective temperature (Grandi and Hawley 1978; Grandi 1975) and by optical observations at positions of different ionization within the same nebula (Peimbert and Torres-Peimbert 1977). The second assumption is premised on calculations which indicate that ionizing stars hotter than 37,000 K, assumed to be the case for the HII regions in this study, will maintain both oxygen and nitrogen predominantly in the doubly ionized state.

The use of far-infrared fine-structure lines in such a survey has

three significant advantages over their optical counterparts: (1), used together, these lines are largely insensitive to electron temperature, density and clumping, (2), because extinction is negligible beyond 50 μm, they can be used to sample regions at $R_G < 8$ kpc, and (3), unlike O^+, there is no need to correct the line intensities for the effects of dielectronic recombination (see Rubin 1986).

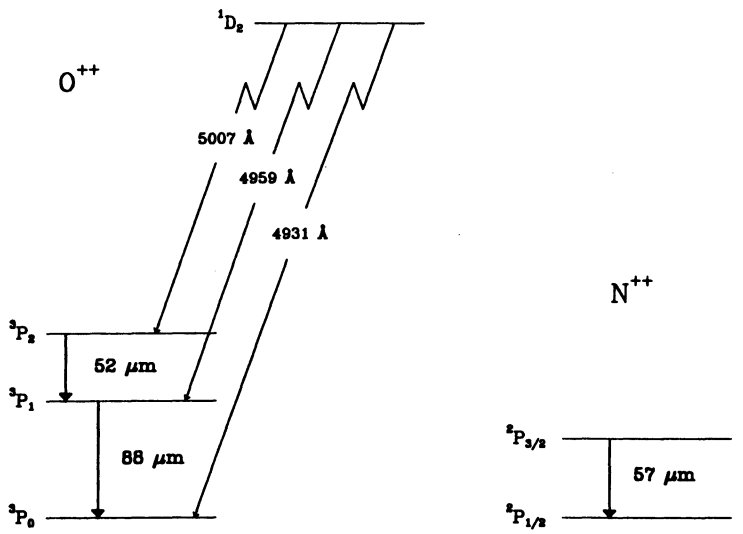

Figure 3. Ground-state energy level diagram for the lowest terms of O^{++} and N^{++}. Optical emission lines of O^{++} are also indicated (the N^{++} $2p^1$ state has no optical transitions).

The procedure for determining the abundance of nitrogen and oxygen from these fine-structure lines is straightforward. The intensity of an optically thin line is simply

$$I_{j\to i} = \frac{h\nu_{ji}}{4\pi} A_{ji} f_j [n_{ion} \ell] \quad , \tag{1}$$

where ν_{ji} is the frequency of the transition, A_{ji} is the probability for spontaneous emission, f_j is the fraction of all ions in the upper state j, n_{ion} is the volume density of the ionic or atomic species, and ℓ is the length of the emitting region along the line of sight. When two fine-structure lines from the same ion are available, the ratio of line intensities reduces to

$$\frac{I_{j\to i}}{I_{k\to j}} = \frac{\nu_{ji} A_{ji} f_j}{\nu_{kj} A_{kj} f_k} = \text{constant} \times (f_j/f_k) \quad , \tag{2}$$

https://doi.org/10.1017/S0074180900153951 Published online by Cambridge University Press

which is independent of source geometry and ionic abundance. Instead, the intensity ratio is a function of the fractional populations of the j and k ground-state levels, f_j/f_k, which is dependent almost exclusively on electron density and only weakly on temperature. Thus, for example, the ratio of the [OIII] 51.82 to 88.35μm line intensities can be used to determine n_e from which the fractional population of the $^2P_{3/2}$ and $^2P_{1/2}$ ground-state levels of N^{++} can easily be calculated. The abundance ratio then follows directly

$$\frac{[N^{++}]}{[O^{++}]} = \frac{(\nu_{ji} A_{ji} f_j)_{O^{++}}}{(\nu_{ji} A_{ji} f_j)_{N^{++}}} \left[\frac{I_{57.3\mu m}}{I_{51.8 \text{ or } 88.3\mu m}}\right], \quad (3)$$

where either [OIII] fine-structure line can be used. Using a procedure similar to the one outlined above, Dinerstein et al. derive the results shown in Figure 4.

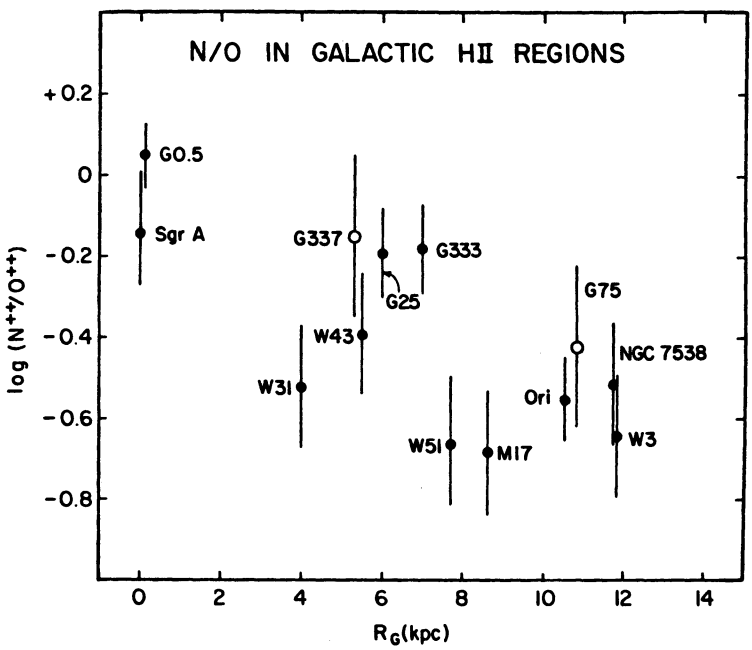

Figure 4. Results of N/O abundance survey of the galactic plane. Filled circles are regions for which the [OIII] 88 and 52μm and [NIII] 57μm lines were observed and n_e determined; regions for which only one [OIII] line and [NIII] were observed are marked by open circles (from Dinerstein et al. 1984).

Their preliminary conclusions are that the N/O abundance ratio is 2 to 3 times greater in the inner galaxy than in the solar neighborhood and

https://doi.org/10.1017/S0074180900153951 Published online by Cambridge University Press

that there is evidence for a secondary peak in the N/O ratio corresponding to the 5 kpc ring. For $R_G > 7$ kpc, the FIR and optical data are consistent and imply a constant N/O ratio. Overall, Dinerstein et al. find an average slope in the N/O ratio of $d\log(N/O)/dR_G = -0.5$ dex kpc^{-1}.

III. FIR/SMM STUDIES OF MOLECULAR CLOUDS

The [OI] 63.18 and 145.53μm and the [CII] 157.74μm lines (see Figure 5) are particularly useful for studying the gas outside of HII regions because: (1) O° and C$^+$ are the dominant states of gaseous oxygen and carbon in the interstellar medium, (2) these lines can be used to measure densities between $\sim 10^2$ and 10^6 cm^{-3}, and (3) the low excitation temperature (< 350 K) of the fine-structure levels makes these lines good probes of temperature below 1000 K. The first observation of the [OI] 63.18μm ground-state fine-structure line from Orion and M17 by Melnick et al. (1979) detected the presence of a component of the interstellar medium intermediate in temperature between the hot (10^4 K), fully ionized gas within HII regions and the cold (< 80 K) molecular gas found in the cores of molecular clouds. Subsequent measurements of the [CII] 157.74μm fine-structure line in Orion, NGC 2024, and M17 (Russell et al. 1980; Russell et al. 1981; Kurtz et al. 1983) substantiated the existence of a significant amount of gas in the range of 100 to 1000 K.

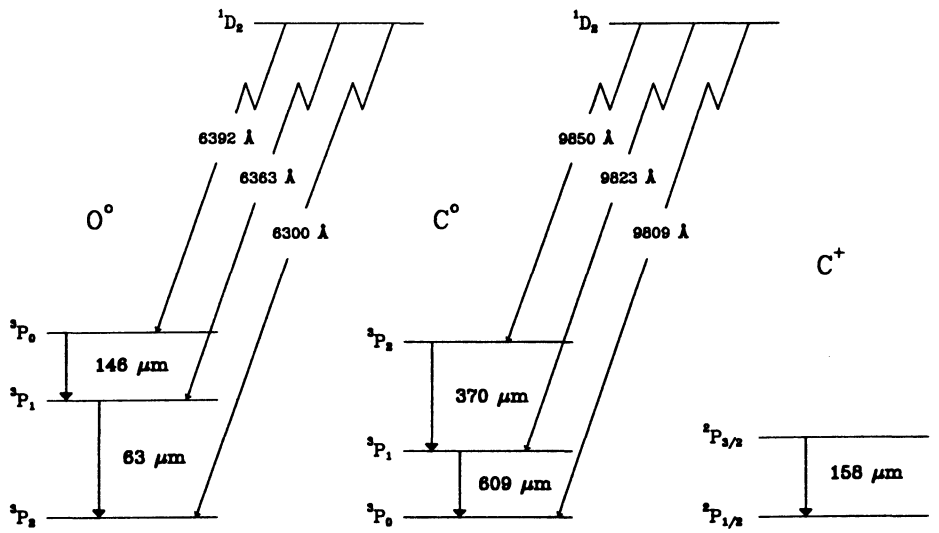

Figure 5. Ground-state energy level diagram for the lowest terms of O°, C°, and C$^+$. Optical and near-infrared emission lines of O° and C° are also shown (the C$^+$ $2p^1$ state has no optical or near-infrared transitions).

https://doi.org/10.1017/S0074180900153951 Published online by Cambridge University Press

To date, the [OI] 63.18 and 145.53μm and the [CII] 157.74μm lines have been observed in a number of HII regions, planetary nebulae, the galactic center, and other galaxies (see Genzel and Stacey 1985, for a recent compilation of the sources observed), with the common result that the gas giving rise to these lines is characterized by densities between 10^4 and 10^5 cm^{-3} and temperatures in excess of 200 K.

This [OI] and [CII] emission is thought to originate from a photodissociation region that is established at the surface of a molecular cloud illuminated by far ultraviolet (FUV) radiation. According to the recent model by Tielens and Hollenbach (1985), FUV ($1101 < \lambda < 912$ Å) photons escaping the ionized gas create a hot (100 - 1000 K) layer of atomic gas between the HII region and an adjacent molecular cloud. At depths into the cloud corresponding to $A_v \leq 3$, FUV photons absorbed by dust grains cause the photo-ejection of electrons which in turn heat the gas. This gas is then cooled by [OI] 63μm and [CII] 157μm line emission. Deeper into the molecular cloud, i.e. $3 \leq A_v \leq 4$, gaseous carbon is predominantly in the form of C and CO. Within this region, the warm (50 - 100 K) gas is largely heated by photoelectrons from dust grains, but is now cooled primarily by rotational lines from CO. The structure of this photodissociation region is shown in Figure 6.

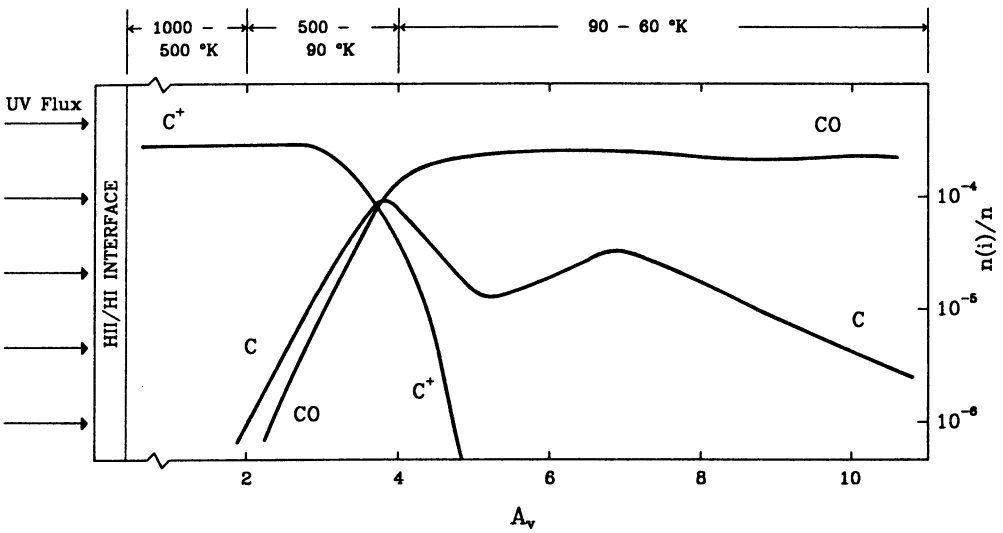

Figure 6. A schematic drawing of a photodissociation region (after Tielens and Hollenbach 1985).

Strip scans made across the ionization front/molecular cloud interface in M17 and S140 in the [CI] 609.14μm line and the ^{12}CO J = 1 → 0 line by Keene et al. (1985) reveal the presence of significant column densities of neutral carbon deep into the molecular clouds in both

https://doi.org/10.1017/S0074180900153951 Published online by Cambridge University Press

sources. This finding contradicts the predictions of the photodissociation models which place most of the CI on cloud edges nearest the HII regions. In M17, CI column densities between 10 and 20% that of CO are found over 60 magnitudes of visual extinction into the molecular gas, while in S140, CI column densities between 13 and 24% that of CO are found ~ 30 magnitudes into the molecular cloud (see Figure 7).

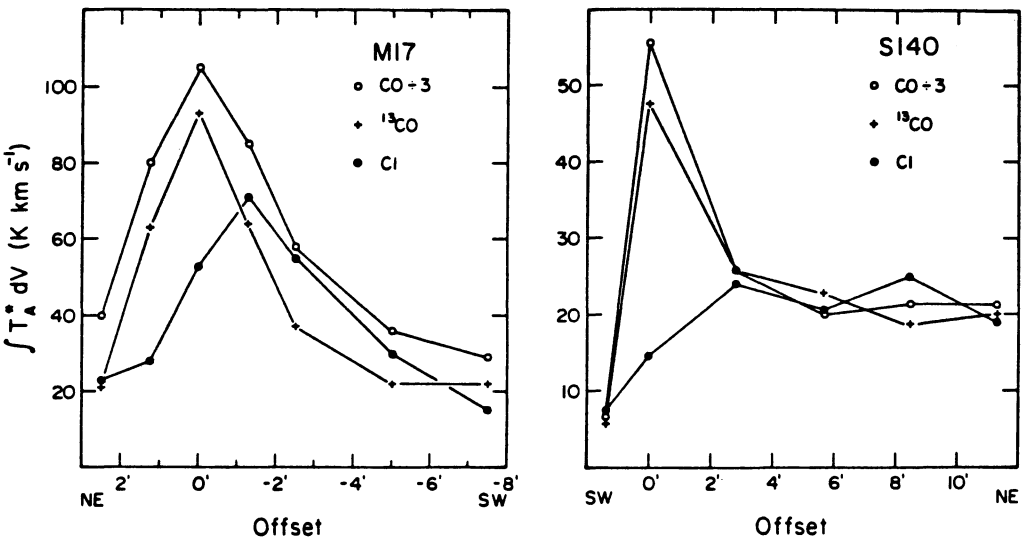

Figure 7. Comparison of CI and CO antenna temperatures in M17 and S140 integrated over velocity. The ionization front is to the left in both plots (from Keene et al. 1985).

A number of carbon chemistry models have been proposed to account for the large abundances of CI. These models, reviewed by Keene et al. (1985; see references therein), include: (1) time-dependent chemistry, in which it is suggested that the time-scale for conversion of CI to CO in the cloud core exceeds the age of the clouds observed, (2) dynamical-chemical models in which the conversion of CI to CO preferentially occurs at high densities, a state achieved only during the last phases of cloud collapse, (3) turbulence, in which cells of gas from the interior of the molecular cloud are constantly exchanged with gas relatively abundant in atomic carbon from the cloud surface, (4) production of CI in the cloud interior through photodissociation of CO by either UV photons generated by internal shock waves and/or cosmic ray excitation of Lyman and Werner bands of H_2, or X-rays from embedded T Tauri and other pre-main-sequence stars, and (5) residual atomic carbon resulting from a C/O abundance ratio > 1 in dense clouds. None of these scenarios are without their drawbacks and an explanation of the [CI] 609μm results remains a constraint for carbon chemistry models.

https://doi.org/10.1017/S0074180900153951 Published online by Cambridge University Press

IV. POST-SHOCKED REGION

Because shock waves both compress and heat the gas as they propagate, conditions immediately behind shock fronts facilitate a large number of chemical reactions that are not favored in the colder, less dense, unshocked gas. The ultimate products of many of the proposed chemical networks, however, depend on the densities and temperatures in the post-shocked region. For this reason, the results of recent FIR/SMM observations of post-shocked gas are of particular interest to those seeking to model the chemical processing that occurs in the wake of shock waves.

Soon after the detection of shock-excited molecular hydrogen from Orion in the mid-1970's, it was recognized that the high-J transitions

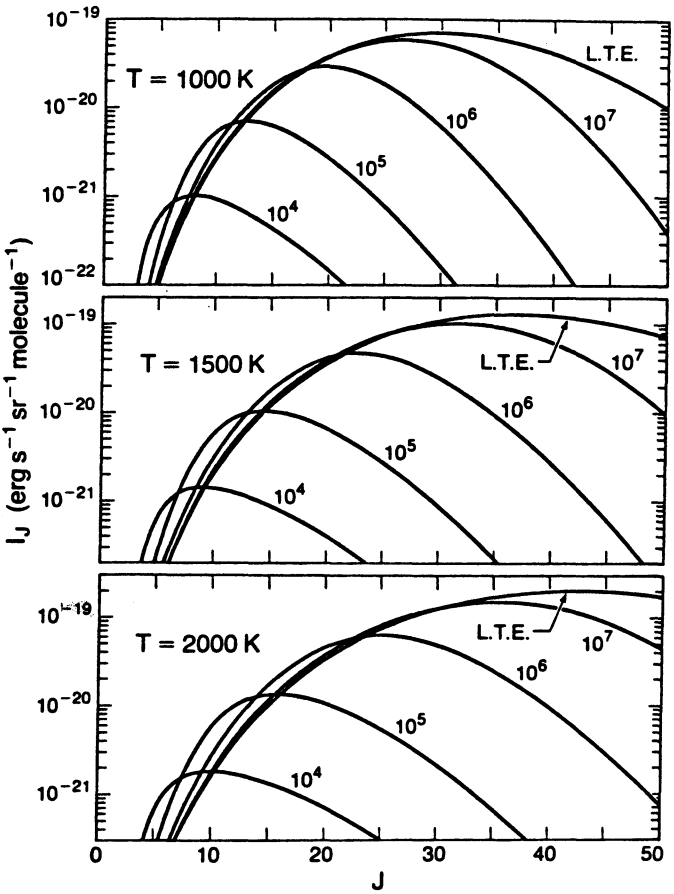

Figure 8. Line emission coefficient I_J for the CO rotational transitions $J \rightarrow J-1$ (from McKee et al. 1982).

https://doi.org/10.1017/S0074180900153951 Published online by Cambridge University Press

of CO could also be used to study the post-shocked gas. These CO lines are unaffected by such complications as variable extinction across the source and the competing effects of fluorescence that affect the near-infrared lines of H_2. Figure 8 shows a plot of CO line emission coefficients as functions of temperature, H_2 density, and J-value as calculated by McKee et al. (1982). Since about 1977, when spectrometers capable of detecting these transitions came into use, 13 different CO rotational transitions between 870 μm (J = 3 → 2) and 77 μm (J = 34 → 33) have been observed, primarily from the Orion Molecular Cloud and the galactic center (e.g. Phillips et al. 1977; Phillips et al. 1980; Goldsmith et al. 1981; Storey et al. 1981; Stacey et al. 1982, 1983; Watson et al. 1985; Harris et al. 1985). Results of these efforts for Orion are shown in Figure 9. As indicated, these data are fit by a two-component model of the post-shocked region in which most of the gas is at 750 K and a density of $\sim 3 \times 10^6$ cm^{-3}, with the remaining 1% of the gas at somewhat higher temperatures (Watson et al. 1985). Compared with the well studied v = 1 → 0 S(1) transition of H_2 at 2.12 μm, which is excited in post-shocked gas of about 2000 K (Beckwith et al. 1978), these CO transitions sample the cooler, downstream gas.

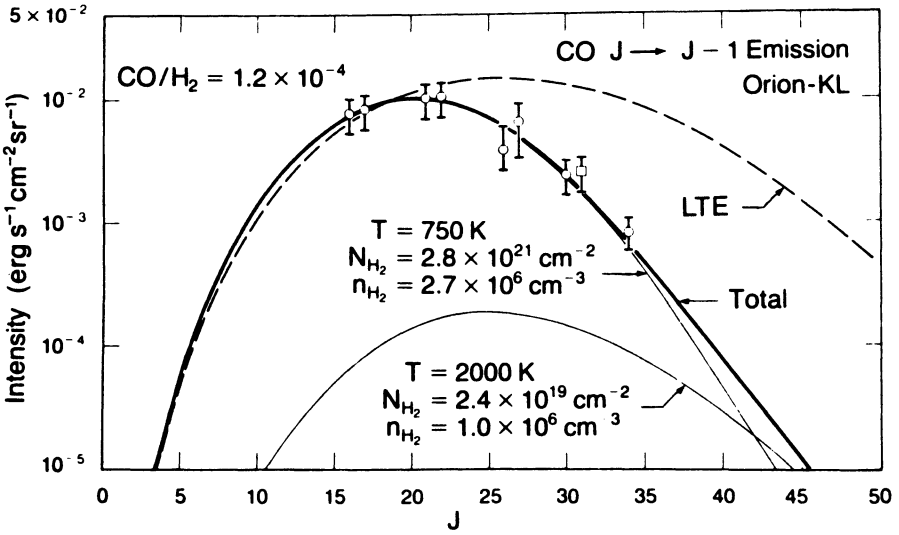

Figure 9. Observed CO line intensities compared to a simple model of the post-shocked gas (from Watson et al. 1985).

More recently, an analogous study of the rotational transitions of OH has begun (see Figure 10). To date, 3 Λ-doublets have been detected from the Orion-KL region: the $^2\Pi_{1/2}$ J = 3/2 → 1/2 doublet at 163.1 and 163.4 μm (Viscuso et al. 1985; Melnick et al. 1986), the $^2\Pi_{3/2}$ J = 5/2 → 3/2 doublet at 119.2 and 119.4 μm (Watson et al. 1985), and

https://doi.org/10.1017/S0074180900153951 Published online by Cambridge University Press

the $^2\Pi_{3/2}$ J = 7/2 → 5/2 doublet at 84.4 and 84.6 μm (Viscuso et al. 1985; Watson et al. 1985). Several possible conclusions can be drawn from both the absolute and the relative OH line intensities. First, the density of the OH emitting region must be ~ 10^7 cm^{-3} or slightly greater. Second, preliminary analysis of the data indicates that the OH emission may arise in either a cool (< 100 K), dense portion of the post-shocked gas, or from an ensemble of ~ 10^7 cm^{-3} clumps, some of which experience radiative excitation of the $^2\Pi_{1/2}$ J = 3/2 level near sources such as IRc 2 or BN. It thus seems that the bulk of the OH emission arises in a different part of the post-shock flow than either high-J CO or 2.12 μm H_2 flux.

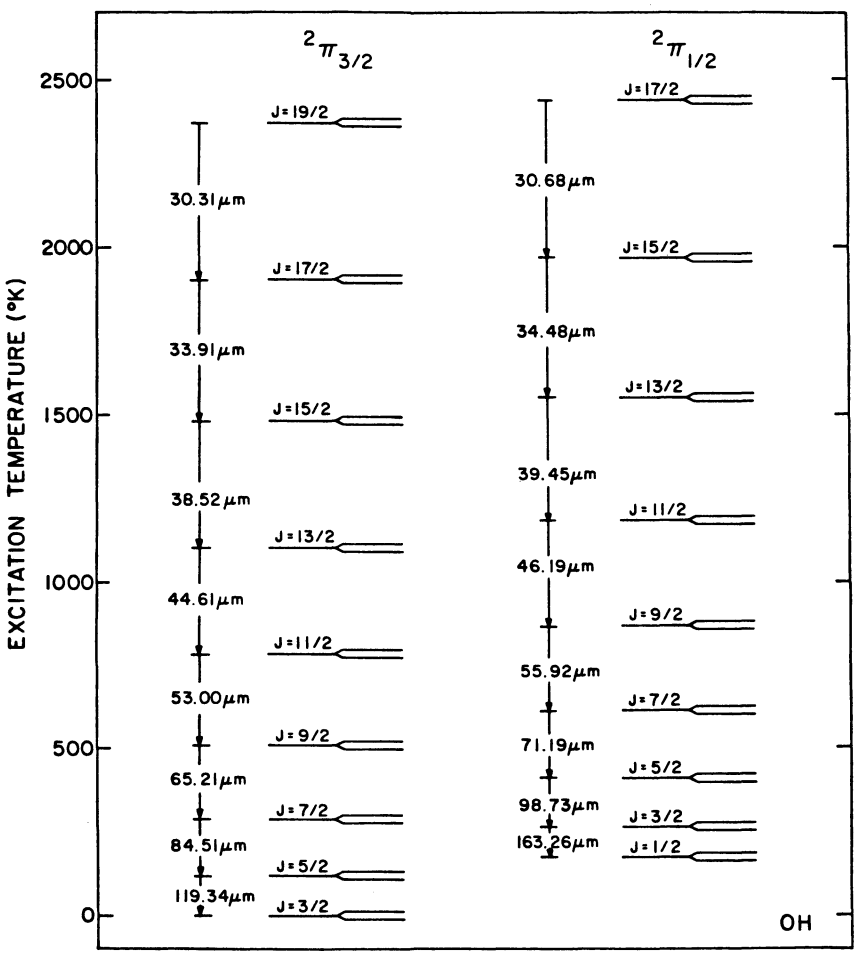

Figure 10. Level structure of OH. The rotational wavelengths shown are averages of the Λ-doublet wavelengths.

https://doi.org/10.1017/S0074180900153951 Published online by Cambridge University Press

Recent improvements in the spectral resolution of instruments operating between 50 and 200 μm permit, for the first time, the measurement of line profiles of several shock-excited lines, such as the [OI] 63.18 μm, the CO J = 16 → 15 transition at 162.81 μm, and the OH $^2\Pi_{1/2}$ J = 3/2 → 1/2 163.1 μm line from Orion-KL. As shown in Figure 11, these lines vary in width from 30 km s^{-1} for [OI] and CO, to 50 km s^{-1} for OH. Beyond the dynamical information inferred from these profiles (see

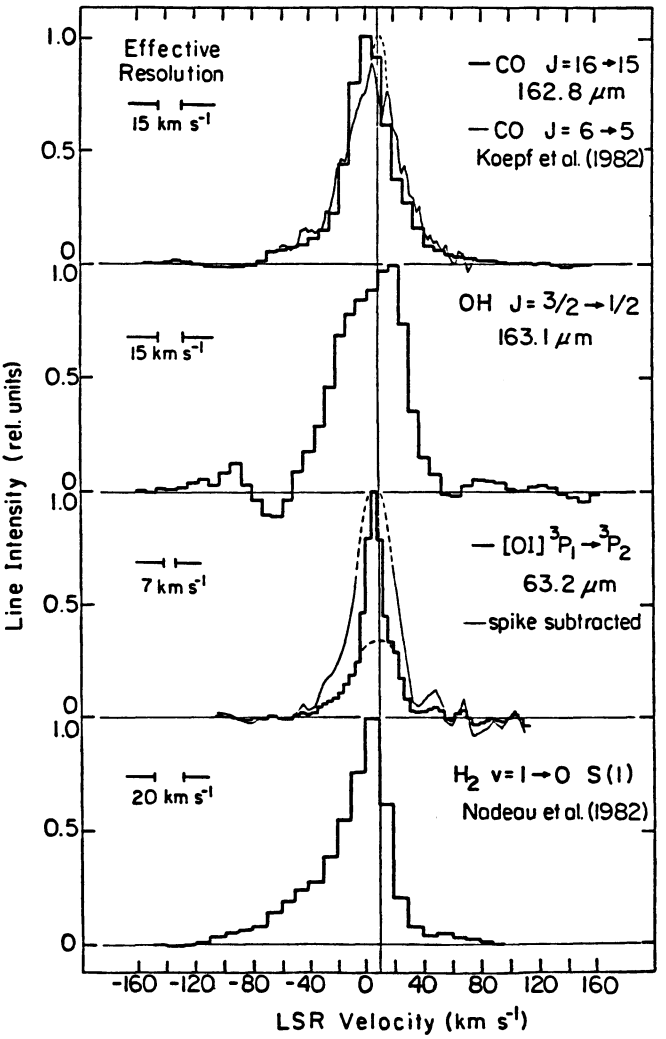

Figure 11. Comparison of line profiles in Orion-KL shock (from Crawford et al. 1986). (a) Deconvolved CO J = 16 → 15 (heavy line) and CO J =6 → 5 (thin line). (b) Deconvolved OH $^2\Pi_{1/2}$ J = $3/2^+ \rightarrow 1/2^-$ profile toward BN-KL. (c) Deconvoled [OI] 63 μm line profile toward H_2 peak 1 (heavy line), and underlying high-velocity emission (thin), after subtraction of the narrow "spike" component. (d) 2.12 μm v = 1 → 0 S(1) H_2.

https://doi.org/10.1017/S0074180900153951 Published online by Cambridge University Press

Crawford et al. 1986), the range of shock velocities implied by these line widths may assist in distinguishing the shock type (J-type or C-type), and thus the conditions responsible for most of the observed emission in Orion-KL. As discussed by Hollenbach (1982) and Chernoff et al. (1982) a strong outflow or wind from BN or IRc2 with velocities of approximately 100 km s^{-1} might be expected to establish a dissociative J-type shock, from which strong atomic emission is predicted. To account for the H_2, CO, and OH emission an additional slower ($\leq$ 50 km s^{-1}), nondissociative C-type shock is invoked (Draine and Roberge 1982; Chernoff et al. 1982). The absence of strong [OI] emission with velocities in excess of 40 km s^{-1}, however, appears to argue against the presence of a strong J-type shock in Orion and more for the presence of just a C-type shock.

ACKNOWLEDGEMENTS

It is a pleasure to thank K. Chance, H. Dinerstein, R. Genzel, J. Keene, R. Rubin and G. Stacey for helpful discussions and permission to present data prior to publication. It is also a pleasure to acknowledge the Smithsonian Institution Foreign Currency Program, NASA contract NAS8-32845 and NASA grant NAG2-311.

REFERENCES

Beckwith, S., Persson, S.E., Neugebauer, G., and Becklin, E.E. 1978, Ap. J. **223**, 464.
Chernoff, D.F., Hollenbach, D.J., and McKee, C.M. 1982, Ap. J. Lett. **259**, L97.
Crawford, M.K., Lugten, J.B., Fitelson, W., Genzel, R., and Melnick, G. 1986, Ap. J. Lett. **303**, L57.
Dinerstein, H., Lester, D., Werner, M., Watson, D., Genzel, R., and Rubin, R. 1984, "Airborne Astronomy Symposium", ed. H.A. Thronson and E.F. Erickson, NASA Conference Publication **2353**, 266.
Genzel, R. and Stacey, G.J. 1985, Proceedings of the German Astronomical Society Symposium on "Interstellar Matter".
Goldsmith, P.F., Erickson, N.R., Fetterman, H.R., Clifton, B.J., Peck, D.D., Tannenwald, P.E., Koepf, G.A., Buhl, D., and McAvoy, N. 1981, Ap. J. Lett. **243**, L79.
Grandi, S.A. 1975, Ap. J. **196**, 465.
Grandi, S.A. and Hawley, S.A. 1978, Pub. A.S.P., **90**, 125.
Harris, A.I., Jaffe, D.T., Silber, M., and Genzel, R. 1985, preprint.
Keene, J., Blake G.A., Phillips, T.G., Huggins, P.J., and Beichman, C.A. 1985, Ap. J. **299**, 967.
Kurtz, N.T., Smyers, S.D., Russell, R.W., Harwit, M., and Melnick, G. 1983, Ap. J. **264**, 538.
Lester, D.F., Dinerstein, H.L., Werner, M.W., Watson, D.M., and Genzel, R.L. 1983, Ap. J. **271**, 618.
McKee, C.F., Storey, J.W.V., Watson, D.M., and Green, S. 1982, Ap. J. **259**, 647.

Melnick, G.J., Genzel, R., Crawford, M.K., and Lugten, J. 1986, in preparation.
Melnick, G., Gull, G.E., and Harwit, M. 1979, Ap. J. Lett. **227**, L29.
Phillips, T.G., Huggins, P.J., Neugebauer, G., and Werner, M.W. 1977, Ap. J. Lett. **217**, L161.
Phillips, T.G., Kwan, J., and Huggins, P.J. 1980, I.A.U. Symposium #87, 21 (Interstellar Molecules, Reidel).
Rubin, R.H. 1986, preprint.
Russell, R.W., Melnick, G., Gull, G.E., and Harwit, M. 1980, Ap. J. Lett. **240**, L99.
Russell, R.W., Melnick, G., Smyers, S.D., Kurtz, N.T., Gosnell, T.R., Harwit, M., and Werner, M.W. 1981, Ap. J. Lett. **250**, L35.
Stacey, G.J., Kurtz, N.T., Smyers, S.D., Harwit, M., Russell, R.W., and Melnick, G. 1982, Ap. J. Lett. **257**, L37.
Stacey, G.J., Kurtz, N.T., Smyers, S.D., and Harwit, M. 1983, M.N.R.A.S. **202**, 25p.
Storey, J.W.V., Watson, D.M., Townes, C.H., Haller, E.E., and Hansen, W.L. 1981, Ap. J. **247**, 136.
Tielens, A.G.G.M. and Hollenbach, D. 1985, Ap. J. **291**, 722.
Traub, W.A. and Stier, M.T. 1976, Appl. Optics **15**, 364.
Viscuso P.J., Stacey, G.J., Fuller, C.E., Kurtz, N.T., and Harwit, M. 1985, Ap. J. **296**, 142.
Viscuso, P.J., Stacey, G.J., Harwit, M., Haas, M.R., Erickson, E.F., and Duffy, P.B. 1985, Ap. J. **296**, 149.
Ward, D.B., Dennison, B., Gull, G., and Harwit, M. 1975, Ap. J. Lett. **202**, L31.
Watson, D.M., Genzel, R., Townes, C.H., Storey, J.W.V. 1985, Ap. J. **298**, 316.
Werner, M.W., Crawford, M.K., Genzel, R., Hollenbach, D.J., Townes, C.H., and Watson, D.M. 1984, Ap. J. Lett. **282**, L81.
Willner, S.P. 1984, in "Galactic and Extragalactic Infrared Spectroscopy", ed. M.F. Kessler and J.P. Phillips (Dordrecht; Reidel), p. 37.

DISCUSSION

JACKSON: What kind of collisional data are needed for OH?
MELNICK: The collision rates used in the calculation of the level populations of OH have varied by a factor of 2 for some transitions between 1984 and 1985. This uncertainty is reflected in the density we believe is necessary to account for the observed intensity of the OH lines. I cannot tell you, though, where the greatest uncertainties in the rate calculations lie.

VAN DISHOECK: More accurate rates for cross-ladder transitions and

https://doi.org/10.1017/S0074180900153951 Published online by Cambridge University Press

transitions within the doublet $\Pi_{1/2}$ ladder of OH in collisions with H and H_2 are needed for temperatures up to 1000 K.

GLASSGOLD: Could you comment on the general prospects for observing the H_2O molecule in the far-infrared.
MELNICK: Unfortunately, most of the strongest astrophysical lines correspond to the stronger atmospheric absorption lines, making their detection from even airplane altitudes quite difficult. Prospects for detecting H_2O in the far-infrared improve if one looks for shock-excited water, since levels with excitation temperatures of 1000-2000 K are relatively weak in our atmosphere. Moreover, if one observes a source with a large Doppler shift, then attenuation by the corresponding terrestrial absorption feature will be further reduced. These constraints are relaxed or eliminated if a spectrometer is flown aboard a balloon-borne telescope, which typically floats at twice the airplane altitude, or about 28 km, or better still, if a spectrometer is flown in space. As yet, no H_2O transitions between 50 and 700 μm have been observed, but it is hoped that this situation will change in the next few years.

WILLIAMS: I refer to the observations of CI and CO in M17 and some of the possible explanations of the fact that the CI is detected in the interior of the CO. Time dependent chemistry in a static cloud will be inadequate since this would make the clouds too young. In a collapsing cloud, the CO would be in the interior. I infer from this that a dynamical solution is needed. Hartquist et al. are currently preparing such a model.

NORMAN: You mentioned that the atomic N/O ratio can tell you something about the relative numbers of low-mass versus high-mass stars. I wonder what can be concluded from the observed variation by a factor of 2 in the N/O ratio going from the galactic center to the solar neighbourhood?
MELNICK: Beyond confidence in their general result that the N/O abundance ratio increases toward the galactic center, I am unaware of any statement the authors of this study have made concerning the relative number of low-mass and high-mass stars. I should emphasize that the results I presented today are part of an on-going study and I believe that a follow-on paper is in preparation.

https://doi.org/10.1017/S0074180900153951 Published online by Cambridge University Press